

Fast interval velocity estimation via NMO-based differential semblance

Jintan Li* and William.W.Symes, Rice University

Summary

Differential semblance velocity analysis flattens image gathers automatically by minimizing the mean square difference of *neighboring traces* in an image volume. Implementations based on normal moveout correction as “imaging” method are relatively fast, can accommodate arbitrary acquisition geometry, and can be organized to output 1D, 2D, or 3D interval velocity models. Within the limits of its imaging methodology (mild structure, data dominated by primary events), this approach to velocity analysis appears to be robust and effective.

Introduction

Differential semblance velocity analysis (“DSVA”) is an automated approach to prestack migration velocity estimation. Its basis is the observation that pairs of nearby image traces exhibit non-aliased residual moveout, even when the migration velocity is dramatically wrong. Objective measures of residual moveout based on this concept can be optimized with respect to migration velocity to produce objective velocity analyses which flatten image gathers automatically.

Many variants of DSVA have been constructed, based on a variety of prestack imaging methodologies: hyperbolic or ray-trace NMO correction in CMP and plane wave domains, two way reverse time, prestack Kirchhoff, and both shot profile and double square root one way wave equation methods have all been used (Symes and Carazzone, 1991; Gockenbach and Symes, 1999; Symes and Versteeg, 1993; Mulder and ten Kroode, 2002; Shen et al., 2003). All of these methods are limited by the requirements of migration imaging:

- input data must be essentially primaries-only - in particular, multiple reflections must have been effectively suppressed prior to velocity analysis;
- trial velocity models must respect the requirements of the imaging engine, usually amounting to some measure of smoothness, and possible *a priori* bounds, chosen to ensure physical correctness and to control numerical artifacts.

DSVA based on hyperbolic normal moveout suffers from the most stringent applicability limits of any of the methods described above, but is also potentially the fastest, as it relies on the simplest imaging engine. Velocity estimates based on NMO are of reasonable utility in areas of low structural relief, either in themselves or as starting models for more sophisticated model-building exercises.

This paper describes an implementation of hyperbolic

NMO-based DSVA with a number of features intended to assist in its assessment for eventual use in a production environment:

- industry standard data structures for input data and diagnostic output;
- flexible velocity modeling accommodating 1D, 2D, and 3D variation within the limits implicit in the imaging methodology;
- state-of-the-art numerical optimization.

We present velocities and image gathers obtained by NMO-based DSVA applied to two North Sea lines. These two marine 2D examples exhibit common features of DSVA: convergence to reasonable velocity estimates in a small number ($O(10)$) of iterations, each involving an imaging step and some side computations; highly aligned image gathers; agreement with standard velocity analysis; measured degradation in the presence of coherent noise.

Algorithmic Details

NMO-based DSVA has been described a number of times, for example by Gockenbach and Symes (1999). We refer the reader to this paper and others referenced there for details of the basic mathematical formulation. We note that the smoothing operator factor mentioned in these references has proven unnecessary in practice, and is omitted in the implementation described here.

The following subsections discuss several key ingredients of a successful DSVA implementation: data format and preparation, velocity model representation, implementation of the NMO transformation, and numerical optimization.

Data Preparation

Data traces are presorted into CMP gathers. Other attributes which must be correctly defined in each trace are source and receiver x and y coordinates, and source and receiver depths. CMP x and y coordinates (as opposed to CMP index) and (3D) offset are computed from this fundamental data. We also require that the delay after the zero phase of the wavelet be given. If this delay is identified with delay after source initiation, then implicitly a zero-phase source-signature deconvolution is assumed to have been applied to the trace.

We have implemented these requirements using the SEG-Y standard, using utilities from the Seismic Unix (“SU”) package (Cohen and Stockwell, 2003). Necessary attributes correspond to the SU header keys `cdp`, `sx`, `sy`,

Fast Differential Semblance

`gx`, `gy`, `selev`, `gelev`, and `delrt`. We have used an object oriented approach to implementation, so any other data structure assigning the appropriate attributes to traces could be substituted for SEG-Y, at the price of writing appropriate wrapper code.

Velocity Representation

NMO-based DSVa assumes a fixed nodal structure for velocity representation. This placement is a *user decision*, and is static. Research on differential semblance has suggested approaches to automatic and dynamic velocity model definition (Symes, 1999), but this topic remains an area for future research. We require that

- Nodes may be placed arbitrarily on arbitrary vertical lines (“wells”), the wells placed arbitrarily within vertical planes (“sections”), and the (parallel) sections be placed arbitrarily in space;
- Nodal values should be *bounding*, i.e. if each nodal value specifying velocity model v_1 is greater than the corresponding nodal value specifying velocity model v_2 , then at an arbitrary point in space (x, y, z) , $v_1(x, y, z) < v_2(x, y, z)$;
- Velocity functions determined by the construction should be *smooth*, that is, without discontinuities in value or slope that would invalidate the naive geometric optics underlying the convolutional model.

The *Partially Irregular Grid* (“PIGrid”) packages accomplishes all of these goals (Dussaud and Symes, 2005). A PIGrid velocity is actually a function of the space variables, and can be sampled on an arbitrary grid (in fact, at an arbitrary point). For use in optimization, adjoints of the sampling functions are required, and the package provides these as well, along with a simple archival storage formal.

NMO Implementation

The new twist in implementing NMO for automatic velocity analysis is that the *derivative* of the NMO correction with respect to velocity is also needed, along with its adjoint, and regrettably standard packages such as SU do not provide these additional computations. Moreover, implementation as a map between regular grids (t , t_0 , or z) inevitably requires interpolation, which is not *a priori* differentiable due to conditional branches and comparisons which occur in natural interpolation code. We have adopted a local cubic interpolation model which minimizes this difficulty; Mulder and ten Kroode (2002) elected a similar approach to this problem, which also occurs in DSVa based on Kirchhoff migration. We used a binning scheme: CMP x and y coordinates, averaged over CMP bin, are used to assign traces to velocity bins, and the velocity profile at the center of each velocity bin is used to move out all traces assigned to that velocity bin.

Controlling NMO stretch requires that upper and lower bounds on velocity be maintained. We permitted the same number of degrees of freedom (i.e. the same PIGrid) for upper and lower envelope velocities, which are user specified but defaulted to $\pm 10\%$ of the initial velocity estimate during optimization.

Numerical Optimization

We employ the Limited Memory Broyden-Fletcher-Goldfarb-Shanno quasi-Newton algorithm (“LBFGS”), generally considered the most effective modern unconstrained optimization algorithm under the widest variety of circumstances (Nocedal and Wright, 1999). We have used the Rice Vector Library (“RVL”) simulation-driven optimization framework to implement this algorithm. This implementation uses a line search subalgorithm to guarantee a reduction in the objective. The line search monitors the upper and lower velocity envelopes, by means of a distance-to-boundary function which is a generic attribute of the function interface in RVL.

Examples

We provide two examples illustrating the performance of NMO-based DSVa. Both are 2D marine, from the North Sea.

Example 1

This line overlies a nearly layered subsurface to 2 s two-way time. Pegleg multiples from the water bottom are evident, as is clear from Figure 2 left, which displays a CMP from this line. Predictive deconvolution suppresses the peglegs, see Figure 2 right. Suspecting from the near-offset section that the shallow structure underlying this line is laterally homogeneous, we elected to search for a 1D velocity model. We selected 21 CMPs which were then input to NMO-based DSVa. The initial velocity estimate was constant = 1.5 km/s. Approximately 10 iterations of LBFGS produced a reduction of two orders of magnitude in the objective gradient, which was our stopping criterion. Each iteration required several seconds on a relatively new Linux-PC platform; the code was compiled with the gcc 3.3 compiler suite with aggressive floating point optimization. The resulting NMO-corrected CMPs (Figure 1) are well-flattened, validating our lateral homogeneity assumption.

Example 2

This example is taken from the Viking Graben data set (Keys and Foster, 1998). This data exhibits a more complex pattern of multiple reflections, with much stronger surface-related multiples, than does Example 1. We began with data to which hyperbolic Radon transform multiple suppression had been applied. Considerable multiple energy is still evident, but a primary reflection series is made visible by this process. We chose 51

Fast Differential Semblance

CMPs covering the 10 km of line, and input these to NMO-based DSVAs. Approximately 20 steps of LBFGS gave convergence from a constant initial velocity (1.5 km/s), convergence once again being defined as reduction of two orders of magnitude in the gradient. Since the velocity structure is known to be laterally heterogeneous, we used a PIGrid with three wells, each having four velocity nodes. NMO correction at the DSVAs optimized velocity, applied to the input data gathers, produced the data displayed in Figure 3. The generally known structure of this section is evident in Figure 3, and the gathers are roughly flattened. To gauge the degree to which kinematic coherence is achieved, we display one of the input CMPs on the left side of Figure 4, and its NMO correction at optimal DSVAs velocity on the right. Conflicting moveout is clearly visible, presumably resulting from incomplete removal of multiply reflected energy. DSVAs attempts to flatten the entire gather, and reaches a compromise, undercorrecting primary events and overcorrecting multiples - this is its generic behaviour in the presence of conflicting moveout (Gockenbach and Symes, 1999). Figure 5 shows RMS velocities derived from the optimized interval velocities, overplotted on a conventional velocity spectrum from midpoints at the three PIGrid "well" locations. This plot gives another index of velocity fidelity achievable by DSVAs in the presence of coherent noise. Finally Figure 6 shows a densely sampled grey scale plot of the estimated velocity, exhibiting structure consistent with that of the prestack image (Figure 3).

Conclusions

We have described an NMO-based implementation of DSVAs and shown some 2D examples of its use. While less flexible than DSVAs based on migration, this implementation gives reasonable approximate interval velocities from data that fall within its domain of applicability, at low computational cost. The results underline the importance of further research to incorporate more physics, notably multiple reflections, into the theory and practice of automatic velocity estimation.

Acknowledgements

We thank the sponsors of The Rice Inversion Project for their support of this work, and Shell International Research and ExxonMobil Upstream Research Co. for provision of the field data used in the Examples section.

References

- Cohen, J. K., and Stockwell, J. J. W., 2003, CWP/SU: Seismic unix release 37: a free package for seismic research and processing: Center for Wave Phenomena, Colorado School of Mines.
- Dussaud, E., and Symes, W. W., A sparse, bound-

respecting parametrization of velocity models:, Technical Report 05-05, Department of Computational and Applied Mathematics, Rice University, Houston, Texas, USA, 2005.

- Gockenbach, M., and Symes, W., 1999, Coherent noise suppression in velocity inversion: Expanded Abstracts, Society of Exploration Geophysicists, 69th Annual International Meeting.
- Keys, R. G., and Foster, D. J., 1998, Comparison of Seismic Inversion Methods on a Single Real Data Set, Society of Exploration Geophysicists, Tulsa.
- Mulder, W., and ten Kroode, A., 2002, Automatic velocity analysis by differential semblance optimization: Geophysics, **67**, 1184–1191.
- Nocedal, J., and Wright, S., 1999, Numerical optimization: Springer Verlag, New York.
- Shen, P., Symes, W., and Stolk, C., 2003, Differential semblance velocity analysis by wave-equation migration: Expanded Abstracts, Society of Exploration Geophysicists, 73rd Annual International Meeting, 2132–2135.
- Symes, W., and Carazzone, J., 1991, Velocity inversion by differential semblance optimization: Geophysics, **56**, 654–663.
- Symes, W., and Versteeg, R., 1993, Velocity model determination using differential semblance optimization: Expanded Abstracts, Society of Exploration Geophysicists, 63rd Annual International Meeting, 696–699.
- Symes, W. W., All stationary points of differential semblance are asymptotic global minimizers: layered acoustics:, Technical Report 99-29, Department of Computational and Applied Mathematics, Rice University, Houston, Texas, USA, 1999.

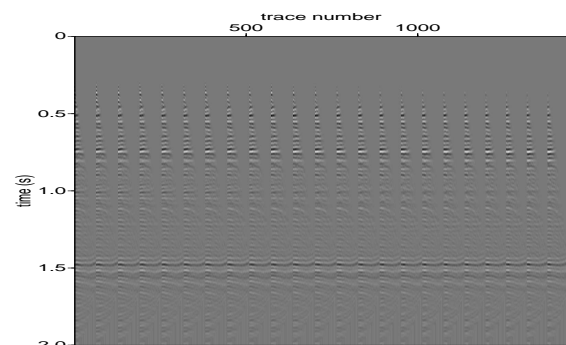


Fig. 1: Example 1: NMO-corrected CMPs

Fast Differential Semblance

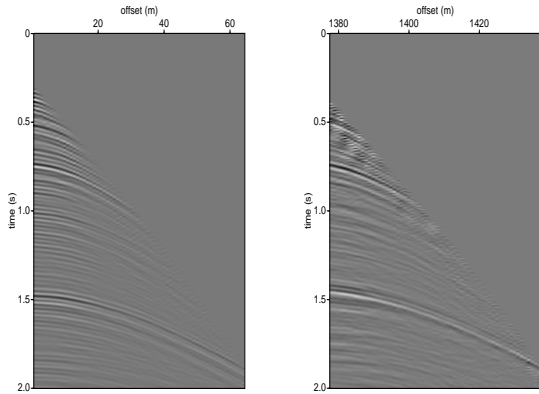


Fig. 2: Example 1: CMP before (left) and after (right) predictive deconvolution.

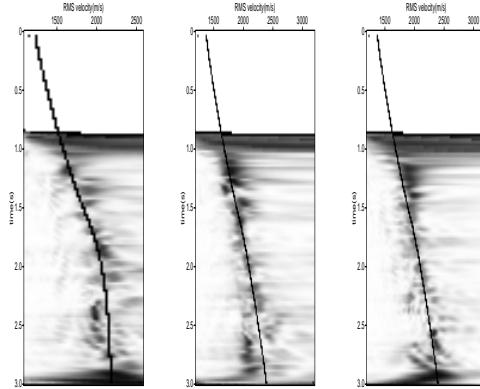


Fig. 5: Example 2: RMS velocities from DSVa interval velocities at three locations in line, plotted over velocity spectra at corresponding CMPs.

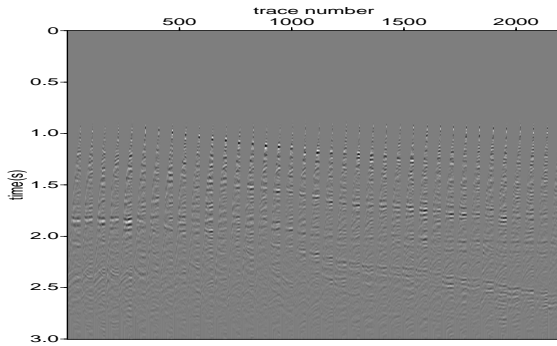


Fig. 3: Example 2: NMO-corrected CMPs

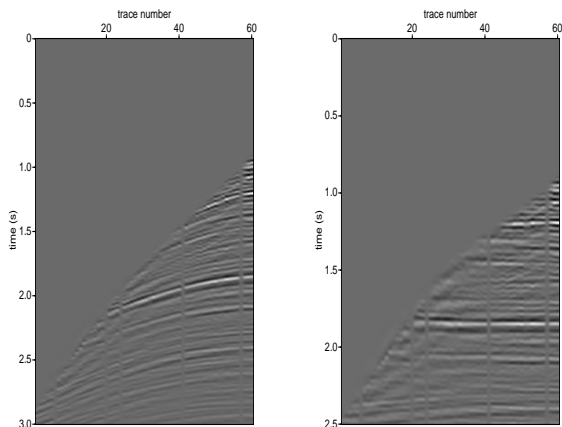


Fig. 4: Example 2: CMP before (left) and after (right) NMO correction with DSVa velocity.

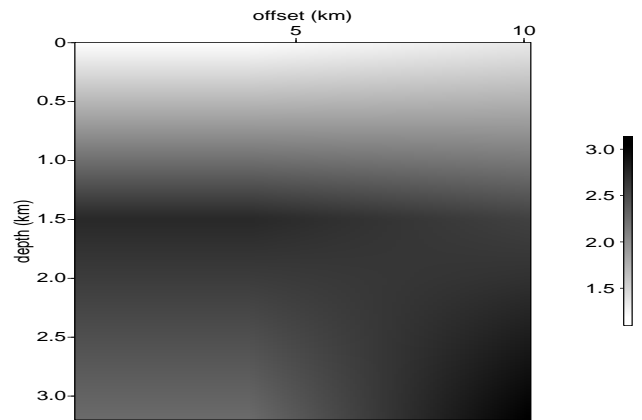


Fig. 6: Example 2: 2D velocity estimated from NMO-based DSVa.